Finite-Element Analysis for Power Electronics EMC Applications

A.M.Sitzia, A.E.Baker, T.W.Preston
GEC ALSTHOM Engineering Research Centre
PO Box 30, Lichfield Road, Stafford, ST17 4LN, U.K.

A.Puzo A.Pons
Alcatel Alsthom Recherche
Route De Nozay, 91460 Marcoussis, France

Abstract — A CAD system for the analysis of power electronic circuits for EMC applications is being developed. The system is based on 3-dimensional finite-element electromagnetic field computations, with the source currents or voltages extracted either from measurements or from standard circuit analysis.

The finite-element solver for this application is configured in terms of magnetic vector potential (A) and modified electric scalar potential (V'), incorporating, unusually, the Coulomb gauge $\nabla.\underline{A}=0$.

Comparisons of computed electromagnetic fields with measurements of fields emitted from a 600V, 300A IGBT switching circuit are reported. Agreement in magnetic field strength is fair (within 8dBμA/m) at the low frequencies (10kHz-20kHz) considered for this paper.

INTRODUCTION

It is becoming increasingly important to be able to predict the electromagnetic field emissions from all kinds of electrical equipment, including power electronic circuits, in order to achieve agreed EMC standards, [1], [2].

This paper reports part of the development of a CAD system which includes circuit analysis (using SABER or other suitable software) to provide source currents and voltages for 3-dimensional finite-element electromagnetic field computation. The paper describes the modelling of an experimental switching circuit, with particular reference to accurate physical representation of the circuit topology. The application described in this paper is to circuits with very fast switching devices (IGBTs), which can produce very high frequency field components.

Comparisons of measured and computed fields from the experimental circuit are presented for illustration.

FINITE-ELEMENT SOLVER

A three-dimensional frequency-domain finite-element solver has been developed for this project, based on magnetic vector potential (A) and modified electric scalar potential (V') as defined in (1) and (2):

$$\nabla \times \underline{A} = \underline{B} \tag{1}$$

$$\underline{E} = -j\omega(\underline{A} + \nabla V') \tag{2}$$

where all other symbols have their accepted meanings. The formulation is based on an energy functional (3) over a volume Ω bounded by a surface area Γ (3):

$$\frac{1}{2}\int_{\Omega}\left[(\underline{H}.\underline{B}) + \frac{1}{j\omega}(\underline{E}.\underline{J})\right]d\Omega + \frac{1}{2j\omega}\oint_{\Gamma}(\underline{E}\times\underline{H})\,d\Gamma \tag{3}$$

where the current density J is taken as:

$$\underline{J} = \sigma\underline{E} + j\omega\underline{D} \tag{4}$$

The Coulomb gauge is applied for uniqueness [3]. The formulation is applied to linear tetrahedral nodal finite elements.

Although an equivalent Galerkin formulation would be also valid, the area term in (3) lends itself elegantly to direct derivation of surface impedance for both thin-skin conducting materials and absorbing boundaries, including free space. For absorbing boundaries, the resulting formulation can be shown to be equivalent to a first-order Engquist-Majda condition [4]. For conducting surfaces, the impedance Z may be written as:

$$Z = (1+j)\sqrt{\frac{\mu_0\mu_r\omega}{2\sigma}} \tag{5}$$

while for absorbing boundaries:

$$Z = \sqrt{\frac{\mu_0\mu_r}{\varepsilon_0\varepsilon_r}} \tag{6}$$

The surface impedance formulation is applied to linear triangular nodal finite elements of any orientation, allowing the use of complex or curved mesh boundaries.

The solver has been tested with a wide range of problems from power-frequency eddy currents to microwave radiation and has been found to be both accurate and robust.

Manuscript received July 10, 1995.

EXPERIMENTAL COMMUTATION CIRCUIT

To validate the application of the solver to power-electronics EMC applications, an experimental forced-commutation switching cell (Figs. 1 and 2) has been constructed, rated at 600V and 300A, to provide empirical data for comparison with computations. In normal operation, switching on the IGBT discharges the main capacitor through the load, then the load current freewheels through the diode when the IGBT is switched off. A typical IGBT current waveform is shown in Fig. 3, with the 10kHz component used as a source current for one of the studies reported in this paper.

FIELD MEASUREMENTS

The experimental cell was placed on an earthed metallic table and all measurements were performed in a semi-anechoic chamber.

Electric and magnetic field strengths have been measured, at several points in space on a vertical plane a little distance in front of the circuit, over a frequency range of 5kHz (which is the fundamental frequency since switching occurred every 200μs) to 7.4MHz. Individual harmonics were extracted by Fourier analysis. Magnetic field measurements were made with a small loop antenna, and electric field measurement with a small ball antenna.

Difficulties encountered include the precise positioning of the measuring antennas and the enforced proximity of data acquisition equipment, as well as numerical errors incurred in calculating magnetic field magnitudes from the three spatial component values or in converting between dB(μA/m) (the units of measurement) and A/m (the SI units used for computation).

Measured magnetic field strength distributions at 10kHz and 20kHz are shown in Figs. 4 and 5, with the circuit outline superimposed for reference.

FIELD COMPUTATION

Finite-element analysis of power electronic circuits is complicated by the fact that the construction and spatial positioning of the components in the circuit depend on factors other than its electromagnetic functioning, unlike, for example, an electrical machine or a microwave circuit.

For example, the heatsink shown in Fig. 1 has primarily a thermal function, but its presence can significantly affect the fields emitted from the circuit. It is necessary, therefore, to construct an accurate solid model of the circuit which includes all electromagnetically significant structures.

The finite-element mesh of the solid model of the commutation cell is shown in Fig. 6. It had 18685 nodes (with 4 complex variables per node), 98100 tetrahedral elements and 4376 triangular surface elements. Since low frequencies were considered initially, the mesh was bounded by Dirichlet conditions a good distance from the circuit and an equipotential plane representing the earthed metal table under the circuit.

The field sources were modelled as a network of complex current vectors, for which the magnitudes and relative time-phases were derived from Fourier analyses of current waveforms measured on the experimental cell. Waveforms derived from circuit analysis could equally have been used.

Figs. 7 and 8 show computed magnetic field strength distributions at 10kHz and 20kHz on a slice through the mesh corresponding to the measurement plane, again with the circuit outline superimposed for reference. Agreement with measurements is good both in general distribution and in magnitude.

The studies at 10kHz and 20kHz took 7800 and 8000 c.p.u. seconds respectively on a SunSPARC20 workstation, with about 100MBytes of memory employed in the computations.

CONCLUSIONS

The initial results presented in this paper serve to illustrate a stage in the development of a CAD system for power electronics EMC applications. They show that reasonable electromagnetic field computations can be achieved even with fairly crude circuit models, using measured or calculated currents as sources.

Further work will refine the modelling of such circuits, exploring the higher frequency components of emitted fields, and develop the link between circuit and field analyses.

The finite-element solver developed for this work has further application over a wide range of eddy-current and wave problems.

REFERENCES

[1] R. Laroussi, G.I. Costache, "Finite Element Method Applied to EMC Problems", *IEEE Trans. Electromagn. Compat.*, Vol. 35, No. 2, pp. 178-184, 1993

[2] D.S. Dixon, M. Obona and N. Schade, "Finite Element Analysis (FEA) as an EMC Prediction Tool", ", *IEEE Trans. Electromagn. Compat.*, Vol. 35, No. 2, pp. 241-248, 1993

[3] O. Biro, K. Preis, "On the use of the magnetic vector potential in the finite-element analysis of three dimensional eddy currents", *IEEE Trans. Magn.*, vol. 25, no. 4, pp. 3145-3159, 1989.

[4] B. Engquist, A. Majda, "Absorbing boundary condition for the numerical simulation of waves", *Mathematics of Computation*, vol. 13, no. 139, 1977.

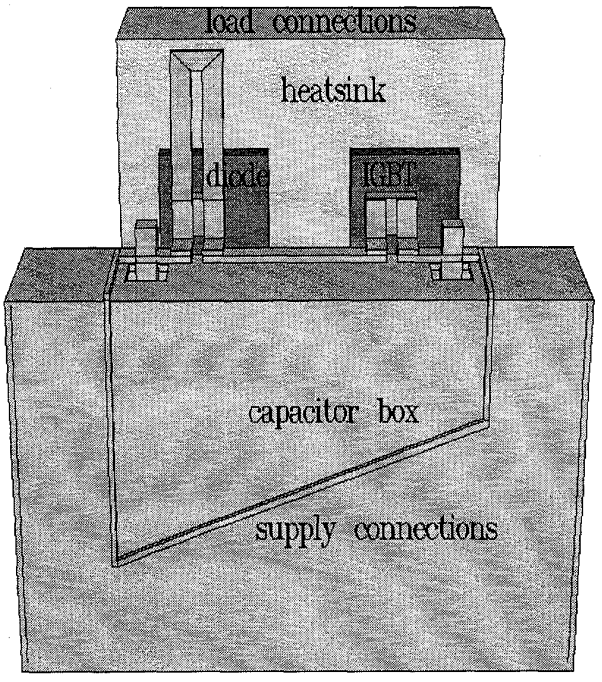

Fig. 1. Layout of experimental switching cell.

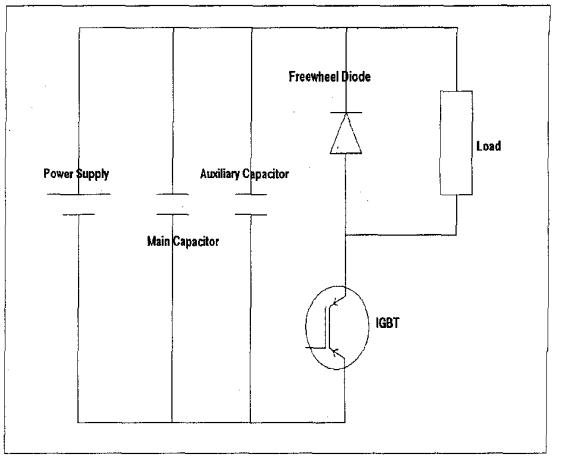

Fig. 2. Schematic of experimental switching circuit.

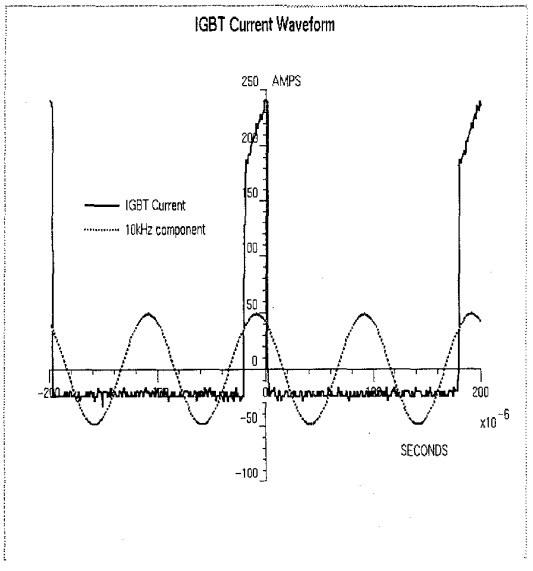

Fig. 3. Example current waveform from experimental circuit.

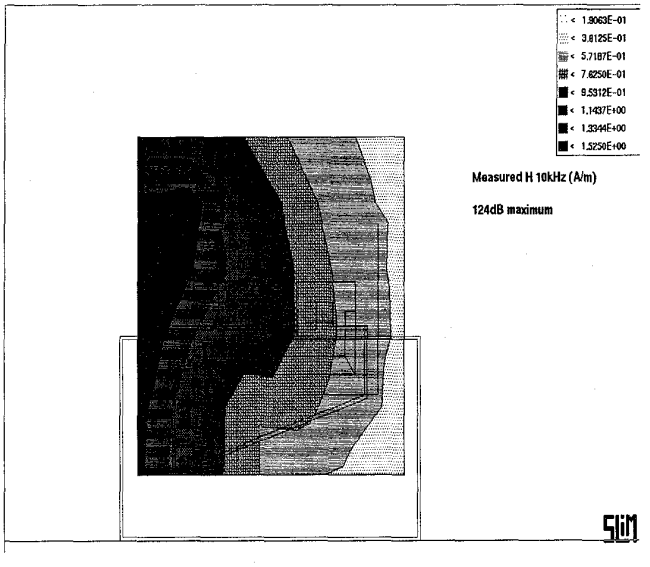

Fig. 4. Measured Magnetic Field Contours at 10kHz.

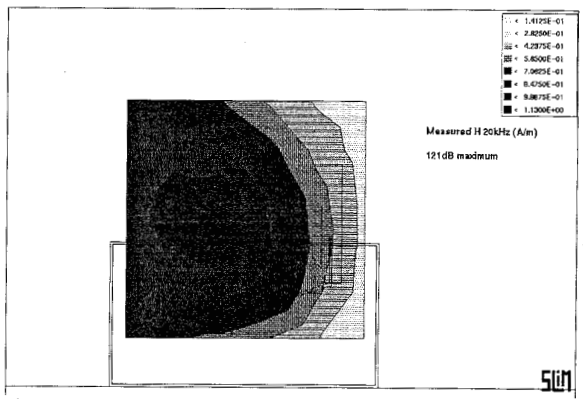

Fig. 5. Measured magnetic field contours at 20kHz.

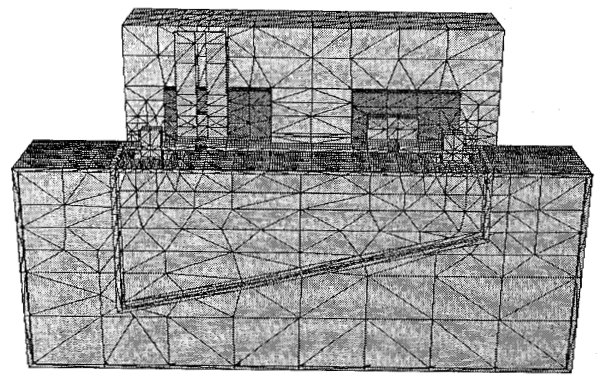

Fig. 6. Finite element mesh for experimental switching cell.

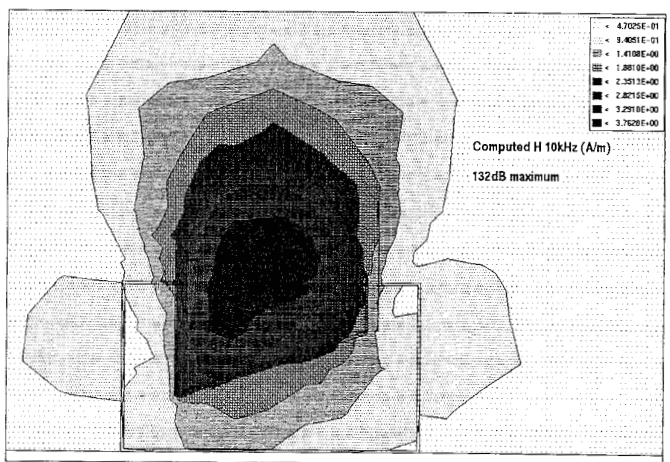

Fig. 7. Computed magnetic field contours at 10kHz.

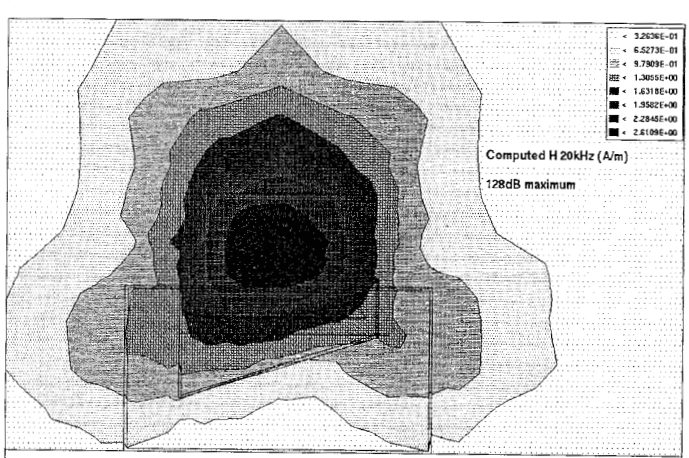

Fig. 8. Computed magnetic field contours at 20kz.